New salicylaldoximato-borate ligands resulting from anion hydrolysis and their respective copper and iron complexes

View Article Online
View Journal

Dalton Transactions

An international journal of inorganic chemistry

Accepted Manuscript

This article can be cited before page numbers have been issued, to do this please use: S. Woodhouse, N. De Silva, G. B. Jameson, D. Cutler, S. Sanz, E. K. Brechin, C. G. Davies, G. N. L. Jameson and P. Plieger, *Dalton Trans.*, 2019, DOI: 10.1039/C9DT01968E.

ROYAL SOCIETY OF CHEMISTRY

rsc.li/dalton

View Article Online
DOI: 10.1039/C9DT01968E

Journal Name

ARTICLE TYPE

Cite this: DOI: 00.0000/xxxxxxxxxx

New salicylaldoximato-borate ligands resulting from anion hydrolysis and their respective copper and iron complexes

Sidney S. Woodhouse,[a] D. Nirosha T. De Silva,[a] Geoffrey B. Jameson,[a] Daniel J. Cutler,[b] Sergio Sanz,[b] Euan K. Brechin,[b] Casey G. Davies,[c] Guy N. L. Jameson,[d] and Paul G. Plieger*[a]

Received Date
Accepted Date

DOI: 00.0000/xxxxxxxxxx

Anion hydrolysis reactions between salicylaldoximato ligands (**L'** - **L"'**) and copper and iron BF_4^- metal salts, have resulted in the formation of new salicylaldoximato borate containing transition metal complexes: $[Fe_2(\mathbf{L'}{+}2H)_2](BF_4)_2(MeOH)_4$ (**C1**), $[Fe_3(\mathbf{L"}{+}4H)(OH)_2(Py)_2](BF_4)_2(H_2O)_2(Py)_2$ (**C2**), and $[Cu_2(\mathbf{L"'}{+}H)_2Cl_2]$ (**C3**). Each of the complexes have been structurally characterised, revealing the indirect role boron plays in the formation of these complexes. For complexes **C1** and **C2**, Mössbauer spectroscopy confirmed the existence of Fe(III) oxidation states. SQUID magnetometry measurements were performed on complexes **C2** and **C3**, revealing the presence of two competing exchange pathways between the three Fe(III) centres in **C2**, with antiferromagnetic exchange dominating. For **C3** weak antiferromagnetic exchange dominated between the two Cu(II) centres.

Introduction

Polynuclear transition metal (3*d*) complexes of salicylaldoxime based ligands, have been studied due to their importance as both biological[1–5] and magnetic materials,[6–9] extractive hydrometallurgy,[10,11] and building blocks for supramolecular structures, such as metal-organic frameworks (MOFs).[12–17]

The appeal of salicylaldoxime based ligands arises from the various different coordination modes, and possible complex topologies. The monoanionic form of basic salicylaldoxime where the phenolate hydrogen is solely lost can form various topologies, with the most common being *cis/trans* mononuclear structures, most commonly used in hydrometallurgy extraction.[10,11,18,19] The dianionic form of simple salicylaldoxime ligands in which both the oximato and phenolate hydrogens are lost can function as both bridging and chelating groups in polynuclear complexes, such as triangular and defective dicubane topologies.[20–24] A key feature of these topologies is the coordination mode of the oximato group, where the N-O atoms form bridges between metal ions, and are capable of introducing structural torsion and interesting physical properties.[25,26] Assembly of supramolecular architectures can depend on many factors such as the nature and/or flexibility of the ligand, geometry of the metal ion, the presence of other molecules and/or anions, and both complexation and recrystallisation conditions.[27]

Since 2016, the use of salicylaldoxime based compounds in *in situ* ligand formation has rapidly grown due to the rise of boron capped/bridged clathrochelate complexes, as this method easily allows for new boron containing ligands to be generated.[12–16,28–30] A clathrochelate complex arises from condensation reactions between di- and tri-oximate species and either boronic acids, boron trifluoride etherates or BF_4^- anions.[14,31,32] There are several examples of 3*d* organometallic complexes in which ions such as fluorine and boron play a significant role in bridging metal ions and capping complexes; these boron species have several applications, such as molecular magnetism, catalysis, and most commonly as building blocks for metallasupramolecular assemblies.[12–17,28–30,32] Suprisingly this method has been under utilised for ligand formation. There are several different types of boron bridged/capped structures known to date, either forming clathrochelate complexes or complexes utilising central bridges, as demonstrated by Tandon *et al.*,[33] who produced a hexanuclear Cu(II) complex with a central μ_6-BO_3^{3-} bridge. This complex differed from other known salicylaldoxime based, boron bridged species, as the borate group bridged metal cations instead of two

[a] *School of Fundamental Sciences, Massey University, Private Bag 11 222, Palmerston North, New Zealand. E-mail: p.g.plieger@massey.ac.nz*
[b] *EaStCHEM School of Chemistry, The University of Edinburgh, David Brewster Road, Edinburgh, EH9 3FJ, UK.*
[c] *Department of Chemistry, University of Otago, PO Box 56, Dunedin 9054, New Zealand.*
[d] *School of Chemistry and Bio21 Molecular Science and Biotechnology Institute, The University of Melbourne, Parkville, Victoria 3052, Australia.*

View Article Online
DOI: 10.1039/C9DT01968E

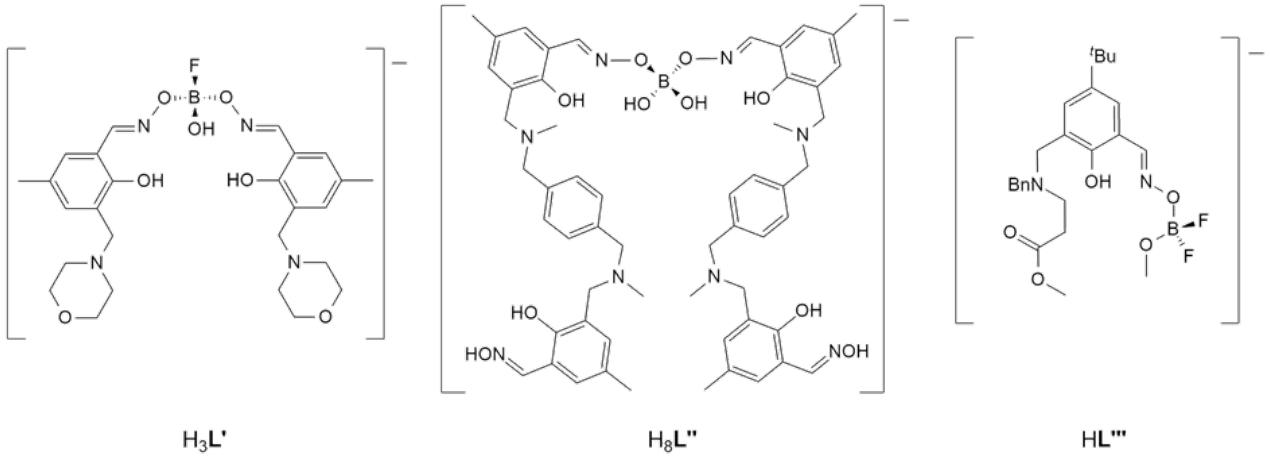

Fig. 1 The chemical structures of the anionic ligands formed *in situ*.

oximato ligands.

We report two new examples of Fe(III) complexes with salicylaldoxime based, fluoroborate and borate bridged ligands formed *in situ*: $[Fe_2(\mathbf{L'}+2H)_2](BF_4)_2(MeOH)_4$ (**C1**) and $[Fe_3(\mathbf{L''}+4H)(OH)_2(Py)_2](BF_4)_2(H_2O)_2(Py)_2$ (**C2**), and the formation of a Cu(II) compound with a terminal difluoromethoxy borane unit, $[Cu_2(\mathbf{L'''}+H)_2(Cl)_2]$ (**C3**).

Results and Discussion

These complexes have been synthesised using ligands that were formed *in situ* by the reaction between either a partial or fully hydrolysed BF_4^- counterion, salicylaldoxime functionalities (Figure 1) and an appropriate metal salt. The readily protonatable amine groups contained within the ligands, were incorporated to add additional support to the resulting copper and iron clusters by the formation of intramolecular hydrogen bonding.

Successful coordination for all three complexes was visually confirmed by the colour of the ligand suspensions changing from pale yellow to either dark maroon (**C1** and **C2**) or dark green (**C3**) solutions.

Solid-state complexes **C1** and **C2** were isolated by the slow evaporation of the filtrate resulting from the reaction between proligands (**L'o** and **L''o** respectively) and $Fe(BF_4)_2{\cdot}6H_2O$ in MeOH at RT. The complex **C3** was isolated by Et_2O vapour diffusion into the reaction mixture of proligand (**L'''o**), $Cu(BF_4)_2{\cdot}6H_2O$ and ammonium chloride at RT.

Both **C1** (dinuclear) and **C2** (trinuclear) feature μ_3-O bridges from the BO_3F and BO_4 bridging groups. In all complexes, oximato oxygen atoms are shared with the tetrahedral boron atoms and not coordinated to the metal centres, a feature commonly seen with known Fe(III)-oximato complexes.[33–35]

Complex **C1** (Figure 2) contains two molecules of the ligand present as **L'**+2H where each ligand has an overall charge of -1 due to the incorporation of the fluoroborate (BO_3F) bridge, deprotonation of phenol groups and protonation of the amino nitrogens. Each Fe(III) ion is bound within a distorted octahedral geometry, with the donor set consisting of one phenolate oxygen atom and one oximato nitrogen from each ligand, and two μ_3-O(BO_3F) atoms, one from each fluoroborate bridge. Each oximato N-O unit forms a bridge between the Fe and B atoms, a feature commonly observed between adjacent metal centres in salicylaldoxime complexes.[33–35] Both the Fe(III) ions and μ_3-O(BO_3F) groups (O13 and O13[a]) sit in the same plane with the boron atoms displaced out of the plane on either side. In addition to the dication, four solvent molecules (MeOH) and two BF_4^- anions were found within the crystal lattice.

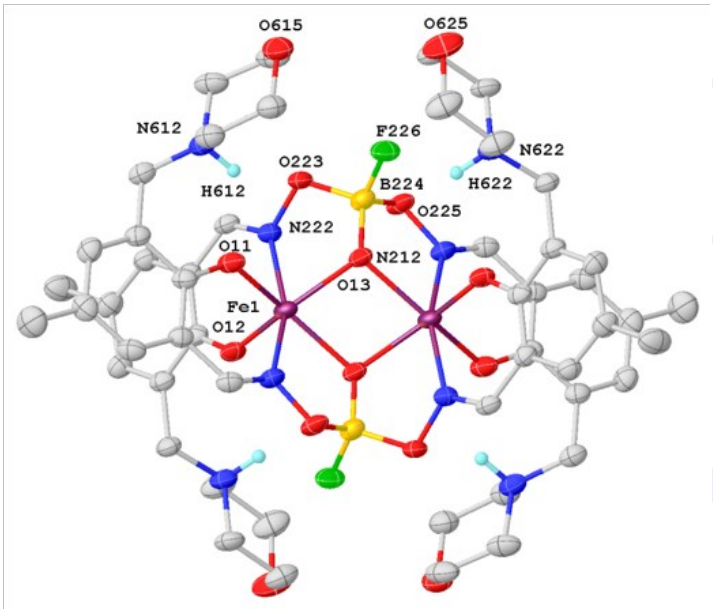

Fig. 2 The X-ray crystal structure of the dication of the complex **C1** (H atoms are omitted for clarity except those participating in hydrogen bonding; H = light blue, B = yellow, C = grey, N = blue, O = red, F = green, Fe = purple). The dication has crystallographic inversion symmetry; The ellipsoids are drawn at the 30% probability level.

In order to confirm the existence of the fluoroborate (BO_3F) bridge in **C1**, bond distances between the oxygen atoms (both oximato and μ_3-O(BO_3F)) and the boron atoms were examined. The average boron-oxygen bond length was 1.440(6) Å, which is significantly longer than the B224-F226 bond length, 1.406(5) Å (see Table 1) confirming the assignment of a μ_3-O(BO_3F) group.[36,37] The average boron-oximato oxygen (O225 and O223)

View Article Online
DOI: 10.1039/C9DT01968E

bond length (1.493(6) Å) of **C1** is longer than both the B-O (μ_3-O(BO_3F)) and B-F bond lengths, and is in agreement with the corresponding average bond length (1.500(5) Å) reported for a related macrocyclic complex containing two CH_3BO_3 bridges by Chaudhuri and coworkers;[32] thus, confirming the assignment as boron-oximato bonds rather than borate bonds. The presence of a single fluorine atom bound to the boron atom in **C1** was confirmed by CHN analysis. The protonated amines within **C1** form intramolecular H-bonds with the phenolate O-atoms (N612···O11, 2.752(4) Å) and intermolecular H-bonds with a solvent (MeOH) molecule (N622···O702, 2.799(4) Å). The MeOH molecule additionally forms intermolecular H-bonds with both the μ_3-O(BO_3F) group (O702···O13, 2.798(4) Å) and the F atom of the fluoroborate bridge (O702···F226, 2.859(5) Å). All H-bonds appear to be of moderate strength, being in the range, 2.5-3.2 Å.[38]

To confirm the Fe-O-B/Fe bridges were indeed μ_3-O(BO_3F) bridges and not μ_3-OH bridges, the Fe-O(BO_3F) (bridging) bond lengths of **C1** were compared with literature examples. The average Fe-O(BO_3F) bond length for **C1** is 2.025 Å, which lies in the range (1.976(2) - 2.067(9) Å) reported by Vasilevsky *et al.*[36] for a Fe_2-μ_3-O(BO_2Ar) species. In further comparison, the range of μ_3-OH bond lengths for the Fe_2-μ_3-OH(BAr_2) moiety by Vasilevsky *et al.*[36] is 2.197(5) - 2.367(2) Å, significantly longer than what was found for the complex **C1**.

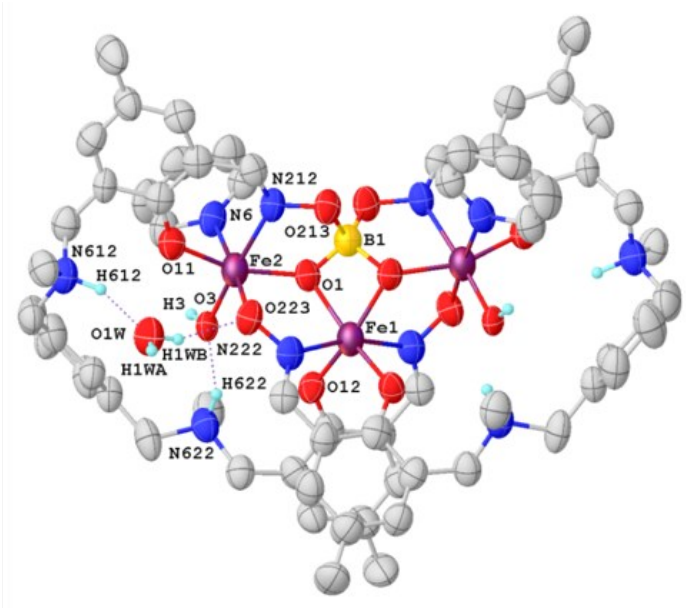

Fig. 3 The X-ray crystal structure of the complex **C2**. The H-bonds are shown as purple dotted lines (H atoms are omitted for clarity except those participating in hydrogen bonding; H = light blue, B = yellow, C = grey, N = blue, O = red, F = green, Fe = purple). The trication has crystallographic two-fold symmetry; The ellipsoids are represented at the 30% probability level.

The complex **C2** is a trinuclear Fe(III) compound that is comprised of one ligand of **L"**+4H, where the four phenolate, two borate and two oximato oxygen atoms are all deprotonated, counterbalanced by the protonation of the four amino nitrogens. Two of the Fe(III) metal cations are in equivalent octahedral coordination environments, comprised of a μ_3-O(BO_4) (borate bridge), a phenolate oxygen atom, a pyridine nitrogen atom and a hydroxo molecule (Figure 3).The hydroxo groups are believed to have come from residual water molecules originating from the hydrated metal salt.[35,39,40] The remaining two donors come from the oximato groups, one oxygen, and one nitrogen from opposite ends of the ligand. The remaining Fe(III) cation sits centrally within the complex in an octahedral coordination environment sharing two μ_3-O(BO_4) atoms (borate bridges), two phenolate oxygen atoms and two oximato nitrogen atoms, one from each end of the ligand (Figure 3). In addition, two BF_4^- ions (each positionally disordered over two sites), two water molecules, and two pyridine molecules (both positionally disordered) exist within the lattice, balancing the overall charge of the complex.

There are several hydrogen bond interactions present within **C2**; these include interactions between lattice water molecules and oximato oxygen atoms (O1w···O223, 2.838(5) Å), and protonated nitrogen atoms (N612···O1w, 2.796(7) Å), which further stabilises the trinuclear iron cluster. Hydrogen bonding is also present between the protonated amines and phenolate oxygen atoms (N612···O11, 2.966(7) Å) and coordinated hydroxo oxygens (N6222···O3, 2.645(6) Å) (see Figure 3 and Table 1).

In **C2**, as with **C1**, the average B-μ_3-O bond length of 1.445(6) Å observed agrees with literature values.[36] The average Fe-μ_3-O(BO_4) bond length of 1.966 Å, however, is significantly shorter than the average Fe-μ_3-O(BO_3F) bond length observed in **C1** as well as in literature.[36] These bridged μ_3-O atoms do not form any hydrogen bonding interactions within the lattice, moreover, the very different coordination mode for the borate bridge in **C2** compared to **C1** leads to a much greater Fe···Fe separation of 3.400 Å for **C2** compared to the 3.141(1) Å for **C1**, allowing shorter Fe-O bonds due to lessened Fe···Fe repulsion. It is not clear if these solid state complexes persist in the solution state.

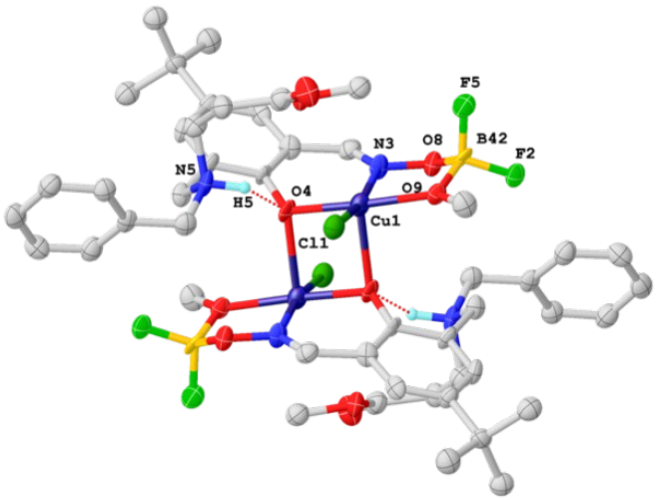

Fig. 4 The X-ray crystal structure of the dication complex **C3** (H atoms are omitted for clarity except those participating in hydrogen bonding; H = light blue, B = yellow, C = grey, N = blue, O = red, F = light green, Cl = dark green, Cu = dark blue). The dication has crystallographic inversion symmetry; The ellipsoids are represented at the 30% probability level.

View Article Online
DOI: 10.1039/C9DT01968E

Table 1 Selected bond lengths (Å) of the complexes: **C1**, **C2**, and **C3**

C1					
Fe1-O11	1.961(3)	Fe1-O12	1.919(3)	Fe1-O13	2.038(3)
Fe1-N212	2.171(4)	Fe1-N222	2.154(4)	Fe1-O13[a]	2.011(3)
F226-B224	1.406(5)	B224-O13	1.440(6)	B224-O225	1.495(5)
B224-O225	1.490(6)	O223-N222	1.390(4)	O225-N212[a]	1.381(4)
C2					
B1-O1	1.445(6)	B1-O213	1.489(7)	Fe1-O1	1.990(4)
Fe1-O12	1.925(4)	Fe1-N222	2.167(4)	Fe2-O1	1.942(4)
Fe2-O3	1.873(3)	Fe2-O11	1.934(4)	Fe2-O223	1.992(4)
Fe2-N6	2.202(5)	Fe2-N212	2.159(5)	O213-N212	1.385(6)
O223-N222[b]	1.380(6)				
C3					
B42-O8	1.468(14)	B42-O9	1.468(15)	B42-F5	1.402(16)
B42-F2	1.413(13)	Cu1-Cl1	2.254(3)	Cu1-O4	1.917(6)
Cu1-O9	1.973(6)	Cu1-N3	1.951(9)	Cu1-O4[c]	2.390(8)
N3-O8	1.382(9)				

[a] = 1-X, -Y, 1-Z; [b] = 3/2-X, 1/2-Y, +Z; [c] = 1-X, -Y, 2-Z

The complex **C3**, contains two molecules of the ligand present as **L'''**+H, where each anionic ligand possesses an overall charge of -1 due to the presence of the terminal difluoromethoxy borane functionality and deprotonation of the phenolate oxygen, which is balanced by the protonation of the amino nitrogen. Each Cu(II) atom lies anti-parallel to one another and is bound within a distorted square pyramidal geometry consisting of one oximato nitrogen, one phenolate oxygen from each ligand, one chloride ion and a methoxy oxygen atom from the terminal difluoromethoxyborane functionality. Each oximic N-O unit, like the previous Fe(III) complexes, forms a bridge between the metal centres and the B atoms. The two phenolic μ_2-oxo bridges, two Cu(II) ions and each oxygen atom contained within the difluoromethoxy borane units all lie within the one plane, with the boron atoms sitting above and below the plane, similarly to **C1**. No additional anions or solvents are found within the crystal lattice. In contrast to complexes **C1** and **C2**, the addition of the difluoromethoxy borane functionality does not bridge two oximato ligands, rather a terminal group is formed together with residual MeOH.

To confirm the existence of the difluoromethoxy borane unit, especially to ensure the BF_2^+ group wasn't a boron dioxide type unit, the B-O bond lengths (oximato (O23) and methoxide (O27)) were compared to that of the B-F bonds. Unfortunately, due to the low resolution of the X-ray data the existence of a BF_2^+ group could not be confirmed by X-ray bond length analysis. Consistent micro-analysis could also not be obtained due to the hydrolytic stability of the complex, therefore the BF_2^+ existence could not be confirmed by elemental analysis. Reinterpretation of the X-ray data with the fluorine atoms replaced with oxygen resulted in a poor fit and non-positive definite atoms. This alone suggested the existence of B-F bonds, but further proof was obtained from a ^{19}F NMR, which clearly showed fluorine to be present with a peak at -150.4 nm. The oximato O-B bond lengths agree with those of similar Cu(II) complexes with hydrolysed BF_2^+ groups; 1.475(5) Å found by Prushan *et al.*[41] and 1.48 Å found by Nanda *et al.*[42] The average B-F bond length (1.35(1) Å) found by Nanda *et al.*[42] is significantly shorter than the average found for the complex **C3**, however, the cause of this could be due to the differences between one being a terminal BF_2^+ group, and the other a bridging group. The average B-F bond length of **C3** was however consistent with the length found for **C1** (see Table 1). Within the complex, a strong intramolecular hydrogen bond (O4···N5, 2.122(8) Å) exists between the phenolate oxygen and protonated amine.[38]

Suprisingly, in all of the complexes, **C1**-**C3**, boron plays an important role in stabilising these low nuclearity Fe(III) and Cu(II) complexes by bridging/binding to the oximato ends of all of the ligands. The crystallographic data for **C1**, **C2** and **C3** can be found in the experimental section.

Mössbauer results and discussion

^{57}Fe Mössbauer measurements were performed on **C1** and **C2** at both low T (4.8 K) and at RT (293 & 290 K). The Mössbauer spectrum of each complex at RT contains a single quadrupole doublet, and in the case of **C1** this is also seen at low T (Figures 5 and 6). The parameters for which the spectra were fit, can be found in Table 2.

Table 2 Fitting parameters of ^{57}Fe on **C1** and **C2** at low temperature and higher temperature (δ = isomer shift, ΔE_Q = quadrupole splitting, Γ = half height line width, I = intensity)

	C1		**C2**
***T* (K)**	4.8	293	290
δ (mm/s)	0.53	0.42	0.39
ΔE_Q (mm/s)	1.19	1.17	0.81
Γ_L (mm/s)	0.33	0.33	0.40
Γ_R (mm/s)	0.33	0.35	0.51
***I* (%)**	100	100	100

Thus, the iron atoms of both complexes belong to the Fe(III) oxidation state, $S = 5/2$, and have octahedral geometry.[43–45] For complex **C1**, the single quadrupole doublet is consistent with crystallagraphic symmetry.[45,46] For complex **C2**, there are two different iron environments, Fe1 and Fe2, in a 1:2 ratio; although sharing the same N_2O_4 suite of ligands, the oximato N atoms are *cis*-related around Fe2 and *trans*-related around Fe1 (Figure 3). Moreover, leading to the expectation of a pair of quadrupole doublets. At RT however, there is notable asymmetry in peak widths,

View Article Online
DOI: 10.1039/C9DT01968E

Γ_L and Γ_R, which strongly suggests two slightly different but unresolved environments for the iron centres. At low T, the Mössbauer spectrum of **C2** shows signs of hyperfine splitting of slowly relaxing Fe(III) centre(s).

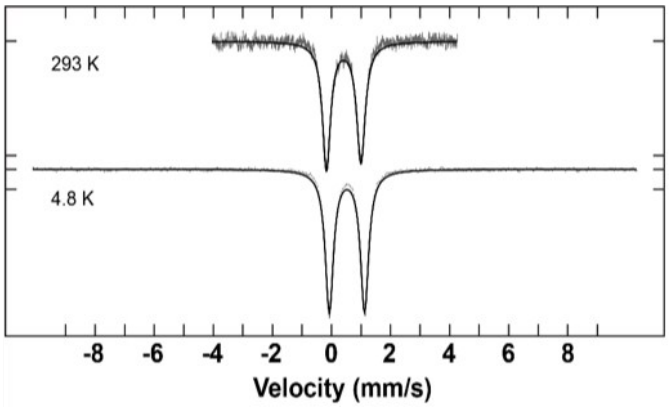

Fig. 5 ^{57}Fe Mössbauer spectra of the complex **C1** overlaid with corresponding fits using the parameters given in Table at high and low temperature.

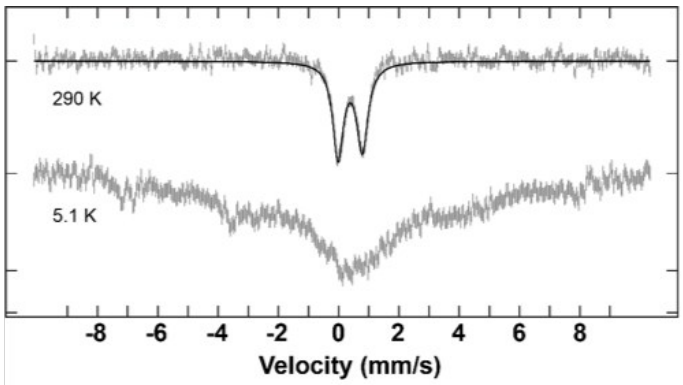

Fig. 6 ^{57}Fe Mössbauer spectra of the complex **C2** at high and low temperature.

Magnetometry

DC (direct current) magnetic susceptibility and magnetisation measurements were performed on **C1**, however the results revealed the presence of a larger than usual paramagnetic impurity (15 %). The measurements suggested strong antiferromagnetic coupling present between the Fe(III) centres, however due to this paramagnetic impurity, a reasonable fit of the magnetic data could not be achieved, and no further magnetic investigations were conducted.

The DC molar magnetic susceptibility, χ_M, of polycrystalline samples of **C2** and **C3** were measured in an applied magnetic field, B, of 0.1 T, over the temperature, T, range of 5-300 K. The experimental results are shown in Figures 7 and 8 in the form of the $\chi_M T$ product, where $\chi_M = M/B$, and M is the magnetisation of the sample. At RT, the $\chi_M T$ product for **C2** of 5.38 cm^3 K mol^{-1} is considerably lower than the value expected for a non-interacting trinuclear Fe(III) complex of $S = 5/2$ spins with $g = 2.0$ (13.125 cm^3 K mol^{-1}). As temperature is decreased the value of $\chi_M T$ decreases rapidly, reaching a minimum of 4.30 cm^3 K mol^{-1} at 80 K, before first rising to a maximum of 4.44 cm^3 K mol^{-1} at $T = 14$ K, then falling to a value of 4.39 cm^3 K mol^{-1} at $T = 15$ K. This behaviour is suggestive of the presence of competing antiferromagnetic exchange interactions between the Fe(III) ions in the trinuclear unit.

For **C3** the RT value of $\chi_M T$ is that expected for two non-interacting Cu(II) ions, assuming $g_{Cu} = 2.2$ (0.91 cm^3 K mol^{-1}). As the temperature is decreased the $\chi_M T$ product decreases very slowly to a value of 0.82 cm^3 K mol^{-1}, before decreasing more rapidly to a value of 0.71 cm^3 K mol^{-1} at $T = 5$ K. This behaviour is suggestive of extremely weak antiferromagnetic exchange between the two Cu(II) ions.

$$\hat{H} = -2\sum_{i,j>i}^{n} \hat{S}_i J_{ij} \hat{S}_j + \mu_B \sum_{i=1}^{n} \vec{B} g_i \hat{S}_i + \sum_{i=1}^{n} D[\hat{S}_{z,i}^2 - \hat{S}_i(\hat{S}_i + 1)/3] \quad (1)$$

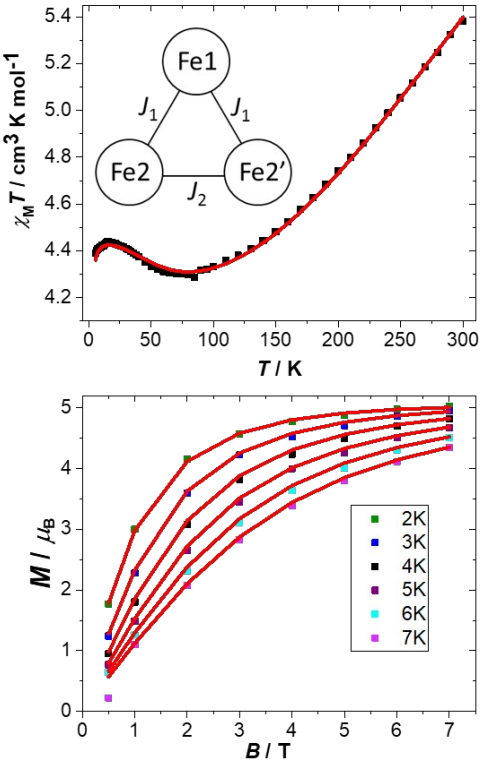

Fig. 7 Plot of $\chi_M T$ vs T (top) for the complex **C2** in the T = 300 - 5 K temperature range in an applied field of B = 0.1 T. The inset shows the triangular model used to fit the experimental data (J_1, Fe1-Fe2, Fe1-Fe2'; J_2 = Fe2-Fe2'). Plot of the VTVB data (bottom) for **C2** in the T = 2 - 7 K and B = 0 - 7 T temperature and field ranges. The solid red lines are a simultaneous fit of the experimental data to spin-Hamiltonian (1). See text for details.

To better define the low T magnetic properties of **C2** and **C3**, low T variable-temperature-and-variable-field (VTVB) magnetisation data were measured in the temperature and magnetic field ranges T = 2 - 7 K and B = 0 - 7 T (Figure 7, bottom; Figure

View Article Online
DOI: 10.1039/C9DT01968E

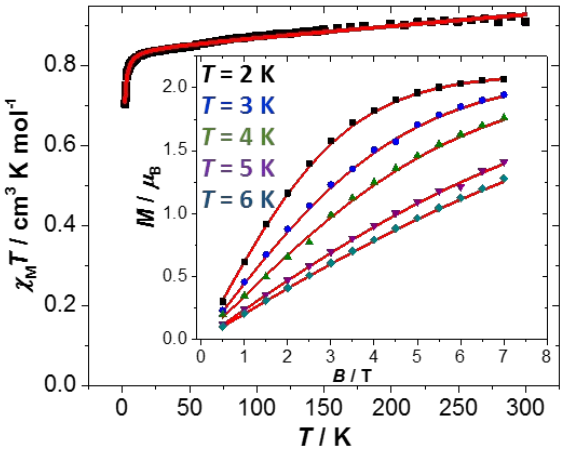

Fig. 8 Plot of $\chi_M T$ vs T for the complex **C3** in the T = 300 - 5 K temperature range measured in an applied field of B = 0.1 T. The inset shows the VTVB data for in the T = 2 - 6 K and B = 0 - 7 T temperature and field ranges. The solid red lines are a fit of the experimental data to the isotropic part of spin-Hamiltonian (1). See text for details.

8, inset). At the highest investigated field (7 T) and the lowest investigated temperature (2 K), the magnetisation of **C2** is 5.03 μ_B (μ_B is the Bohr magneton). A simultaneous fit of the susceptibility and magnetisation data employing spin-Hamiltonian (1) and the (isosceles triangle) model shown in the inset of Figure 7 (with g fixed at g = 2.02) afforded the best fit parameters J_1 = -25.15 cm^{-1} and J_2 = -0.062 cm^{-1}, and D_{Fe} = -0.323 cm^{-1}, with a TIP of 2.42 x 10^{-4} cm^3 mol^{-1}. The fit can be improved somewhat through the inclusion of an intermolecular interaction term, zJ = -0.0069 cm^{-1}. The magnitude of the J_1 exchange interaction is consistent with the coupling expected between two Fe(III) ions connected through one Fe1-O1(B)-Fe2 (~119°) and one Fe1-O223(oxime)-N222(oxime)-Fe2 (~21°) units, with D_{Fe} close to that expected for a distorted octahedral ion.[34,47] The magnitude of the J_2 exchange interaction is, not surprisingly, much weaker than J_1 due to the longer exchange pathway required for coupling. A simultaneous fit of the susceptibility and magnetisation data for **C3** employing the isotropic part of spin-Hamiltonian (1) afforded the best fit parameters J = -0.38 cm^{-1} with g = 2.12, with a TIP = 2.89 x 10^{-4} cm^3 mol^{-1}. The very small value of J is to be expected from a phenoxo-bridged Cu(II) dimer with Cu-O-Cu angles of ~96°, close to the crossover point between ferro- and antiferromagnetic exchange.[48,49]

Conclusions

Anion hydrolysis reactions between the proligands, **L'o** - **L"'o**, and $Cu(BF_4)_2{\cdot}6H_2O$ and $Fe(BF_4)_2{\cdot}6H_2O$ metal salts has resulted in not only the formation of three new Cu(II) and Fe(III) complexes, but also the formation of three new salicylaldoximato-borate ligands (H_3**L'**, H_8**L"**, and H**L"'**) formed *in situ*. The centrosymmetric symmetry and the single crystallograhically unique iron species of the dinuclear iron compound, **C1** are clearly evident by the presence of a single quadrupole doublet at both RT and low T in the Mössbauer spectrum. The isomer shift and quadrupole splitting values indicate that the iron centres belong to the high-spin, +3 oxidation state. The trinuclear iron complex **C2**, which features a borate (BO_4^{3-}) bridge which not only bridges two oximato oxygens but also bridges the iron atoms in both a $\mu_{1,1}$ mode and a $\mu_{1,3}$ mode. Mössbauer spectroscopy measurements of this complex do not resolve the expected pair of quadrupole doublets, however, the apparent single doublet is broad and the line widths of the doublet are significantly different. As with **C1**, the isomer shift and quadrupole splitting values indicate high-spin Fe(III) centres. Dc magnetic susceptibility and magnetisation measurements reveal the presence of strong antiferromagnetic and weak ferromagnetic exchange between the three Fe(III) centres in **C2**. The complex **C3** features two square pyramidal Cu(II) ions each with a terminal difluoromethoxy borane (BF_2OCH_3) group bound via the oximato group of the ligand. Dc magnetic susceptibility and magnetisation measurements reveal very weak antiferromagnetic exchange between the Cu(II) ions in **C3**, consistent with previously published species possessing similar structures. The present study highlights the utility of *in situ* ligand synthesis from anion hydrolysis reactions with salicylaldoximato containing ligands.

Experimental Section

General Details

All reactions were performed under aerobic conditions using chemicals and solvents as received, unless otherwise stated. ^{1}H and ^{13}C NMR spectra were recorded on Bruker Avance 500 and 700 MHz spectrometers, δ values are relative to TMS or the corresponding solvent. ^{19}F NMR was recorded on a Magritek spinsolve benchtop NMR. Mass spectra were obtained using both a Micromass ZMD 400 electrospray spectrometer, and a Dionex UltiMate 3000 spectrometer. IR spectra were recorded on a Nicolet 5700 FT-IR spectrometer using an ATR sampling accessory. UV/Vis spectra were collected using a Shimadzu UV-3101PC spectrophotometer. Conductivity measurements were collected using a Phillips PW9509 conductivity meter. Melting point measurements were collected on a Gallenkamp melting point apparatus. Elemental analyses were determined by the Campbell Microanalytical Laboratory at the University of Otago. Variable temperature, solid-state direct current (dc) magnetic susceptibility data down to 2 K was collected on a Quantum Design MPMS-XL SQUID magnetometer equipped with a 7 T dc magnet at the University of Edinburgh. Diamagnetic corrections were applied to the observed paramagnetic susceptibilities using Pascal's constants. Mössbauer data was recorded on a SEE Co. (Science Engineering and Education Co., MN) spectrometer, equipped with a closed cycle SVT-400 cryostat from Janis Research Co. and SHI (Sumitomo Heavy Industries Ltd.) at the Univeristy of Otago. The data was collected in a constant acceleration mode in a transmission geometry. The isomer shift (zero velocity) of the Mössbauer spectra were determined relative to the centroid of the RT spectrum of a metallic iron foil. The data analysis was performed using the program WMOSS.

View Article Online
DOI: 10.1039/C9DT01968E

Table 3 Crystal data and structure refinement details for complexes **C1**, **C2**, and **C3**

	C1	**C2**	**C3**
Formula	$C_{56}H_{84}B_4F_{10}N_8O_{18}Fe_2$	$C_{76}H_{90}B_3F_8N_{12}O_{14}Fe_3$	$C_{48}H_{64}B_2F_4N_4O_{10}Cu_2$
M_r (g mol^{-1})	1502.25	1747.57	1152.63
T (K)	152	143	103
Crystal system	Triclinic	Orthorhombic	Triclinic
Space group	$P\bar{1}$	$Pccn$	$P\bar{1}$
a (Å)	10.292(5)	15.408(5)	10.042(13)
b (Å)	12.325(3)	19.133(5)	10.282(14)
c (Å)	15.431(5)	30.848(5)	13.683(15)
α (°)	73.437(5)	90	104.670(7)
β (°)	71.084(3)	90	95.931(7)
γ (°)	67.319(5)	90	110.168(8)
V (Å^3)	1679.5(11)	9094(4)	1254.2(3)
Z	1	4	1
$\rho calc$ (g cm^{-3})	1.485	1.276	1.526
μ (mm^{-1})	4.352	4.457	2.678
F (000)	782	3628	598
$\theta_{min}/\theta_{max}$ (°)	13.386/144.096	13.648/117.862	6.83/117.818
Reflections collected	23554	57601	11410
Unique reflections	6229	6442	3489
R_{int}	0.0663	0.1248	0.1932
Data/restraints/parameters	6229/28/491	6442/671/584	3489/150/330
Goodness-of-fit on F^2	1.087	1.080	0.835
Final R_1 ($I > 2\sigma(I)$)	0.0493	0.0861	0.0838
wR_2	0.1403	0.2674	0.2320
Residual difference electron density (e$^-$/Å^3)	0.67/-0.62	0.69/-0.67	0.73/-0.57
CCDC No.	1531607	1543536	1889344

X-ray Crystallography

The X-ray data was collected at reduced temperature on a Rigaku Spider diffractometer equipped with a copper rotating anode X-ray source and a curved image plate detector. Crystals were mounted in Fomblin and transferred into the cold gas stream of the detector and irradiated with graphite monochromated Cu Kα (λ = 1.54187 Å) X-rays. Crystal Clear[50] was utilised for data collection and FS PROCESS in PROCESS-AUTO[51] for cell refinement and data reduction. Solution and refinement was achieved using Olex2.[52] The structures of **C1** and **C2** were solved by direct methods and expanded by Fourier techniques.[53,54] The structure of **C3** was solved using the program Superflip[55–58] and refined using SHELXL[54] in Olex2.[52] Non-hydrogen atoms were refined anisotropically, and hydrogen atoms were placed in calculated positions, and refined by using a riding model with fixed isotropic **U** values. The lattice BF_4^- anions within **C1** are positionally disordered over two sites in a 60 : 40 ratio. For **C2**, both the two lattice BF_4^- anions, and the two lattice pyridine molecules are positionally disordered in a 50 : 50 ratio. Disordered solvent regions in the complex, **C2** were treated in the manner described by Spek[59] as implemented in Olex2,[52] resulting in the removal of 236 e$^-$ per cell. This value approximates to 11 H_2O molecules and seven MeOH molecules per cell (236).

Ligand Syntheses

The starting materials of the multi-step ligand syntheses, 5-methylsalicylaldehyde and 5-*tert*-butylsalicylaldehyde were synthesised as described in the literature.[60] The preparation of 3-(bromomethyl)-2-hydroxy-5-methylbenzaldehyde (**1a**) and 3-(bromomethyl)-2-hydroxy-5-*tert*-butylbenzaldehyde (**1b**) were carried out by the procedures of Wang *et al.*[61] and Meier *et al.*[62] respectively. The preparation of the secondary amine, *N*,*N*'-dimethyl-*m*-xylylenediamine (**2**), oxime precursors and the proligands were carried out according to the method of Stevens and Plieger.[63] The preparation of the secondary amine, *N*-benzyl-β-alanine methylester (**3**) was prepared according to the method of Cruz-Huerta *et al.*[64]

L'a (Precursor for L'o): 2-hydroxy-5-methyl-3-(4-morpholinomethyl)benzaldehyde

Solutions of **1a** (1.27 g, 5.54 mmol) and morpholine (1.31 g, 14.8 mmol) both in dichloromethane (60 mL) were added dropwise to a stirred solution of triethylamine (3.40 g, 14.8 mmol) in dichloromethane (80 mL). The resulting yellow solution was stirred for 24 hours at RT. The solution was washed with deionised water (3 x 100 mL) and the combined organic layers were dried over anhydrous sodium sulfate, filtered and concentrated *in vacuo* to afford a yellow oil (2.99 g, 86%). ^{1}H NMR (500 MHz, $CDCl_3$, TMS): δ 10.21 (s, 1H, C*H*O), 7.41 (d, J = 1.7 Hz, 1H, Ar-*H*(σ-amine)), 7.20 (d, J = 1.7 Hz, 1H, Ar-*H*(σ-oxime)), 3.76 (t, J = 4.8 Hz, 4H, OCH_2), 3.67 (s, 2H, Ar-CH_2N), 2.57 (br s, 4H, NCH_2), 2.30 (s, 3H, CH_3); ^{13}C NMR (125.7 MHz, $CDCl_3$, TMS): δ 192.7, 158.7, 137.1, 129.5, 128.5, 123.4, 122.0, 66.7, 59.0, 53.1, 20.2; IR: $\bar{\nu}$ = 1674 (C=O), 1115 (C-O), 1233 (C-N) cm^{-1}; MS: *m/z* (ESI) 235 [M+H]$^+$; elemental analysis calcd. (%) for $C_{13}H_{17}NO_3$: C 66.36, H 7.28, N 5.95; found: C 66.20, H 7.42, N 6.12.

L'o (Precursor for L'): 2-hydroxy-5-methyl-3-(4-morpholinomethyl)benzaldehyde oxime

A solution of hydroxylamine hydrochloride (2.78 g, 11.8 mmol) in ethanol (100 mL) was neutralised with a solution of potassium hydroxide (0.662 g, 11.8 mmol) in ethanol (100 mL). The filtered

View Article Online
DOI: 10.1039/C9DT01968E

solution was added slowly dropwise to a solution of **L'a** (2.78 g, 11.8 mmol) in ethanol (200 mL) over 30 minutes. The resulting solution was stirred for 24 hours at RT. The pale yellow solution was concentrated *in vacuo* affording an oil, which was redissolved in chloroform (300 mL). This solution was washed with deionised water (100 mL) and the combined organic layers were dried over anhydrous sodium sulfate, filtered and concentrated *in vacuo* to afford a yellow solid, which was further washed with cold ethanol (70 mL). The resulting white powder was dried *in vacuo* for 24 hours (1.25 g, 42%). Mp: 194.5 - 196.5 °C; ^{1}H NMR (500 MHz, d_6−DMSO, TMS): δ 8.28 (s, 1H, C*H*N), 7.22 (d, J = 1.8 Hz, 1H, Ar-*H*(σ-amine)), 6.98 (d, J = 1.8 Hz, 1H, Ar-*H*(σ-oxime)), 3.59 (t, J = 4.6 Hz, 4H, OCH_2), 3.67 (s, 2H, Ar-CH_2N), 2.44 (br s, 4H, NCH_2), 2.03 (s, 3H, CH_3); ^{13}C NMR (125.7 MHz, d_6−DMSO, TMS): δ 153.5, 147.2, 131.7, 127.9, 126.8, 123.1, 118.4, 66.5, 58.7, 53.1, 20.5; IR: $\bar{\nu}$ = 2964 (C-H), 1618 (C=N), 1471 (C-H), 1267 (C-O), 1111 (N-O) cm^{-1}; MS: *m/z* (ESI) 251 $[M+H]^+$; elemental analysis calcd. (%) for $C_{13}H_{18}N_2O_3$: C 62.38, H 7.25, N 11.19; found: C 62.34, H 7.34, N 10.95.

L"a (Precursor for L"o): 3,3'-[1,3-phenylenebis[methylene(methylamino)methylene]]bis[2-hydroxy-5-methylbenzaldehyde]

Solutions of **1a** (1.27 g, 5.54 mmol) and **2** (0.46 g, 2.77 mmol) both in dichloromethane (15 mL) were added dropwise to a stirred solution of triethylamine (1.11 g, 11.0 mmol) in dichloromethane (20 mL). The resulting yellow solution was stirred for 24 hours at RT. The solution was washed with deionised water (3 x 70 mL) and the combined organic layers were dried over anhydrous sodium sulfate, filtered and concentrated *in vacuo* to afford a yellow waxy solid (1.19 g, 92%). ^{1}H NMR (500 MHz, $CDCl_3$, Me_4Si): δ 10.29 (s, 2H, C*H*O), 7.29 (d, J = 2.8 Hz, 2H, Ar-*H*(σ-amine)), 7.28 (s, 1H, Ar-*H*), 7.18 (d, J = 1.8 Hz, 2H, Ar-*H*(σ-oxime)), 3.74 (s, 4H, CH_2N), 3.73 (s, 4H, Ar-CH_2N), 2.57 (br s, 4H, NCH_2), 2.29 (s, 6H, NCH_3), 2.28 (s, 6H, Ar-CH_3); ^{13}C NMR (125.7 MHz, $CDCl_3$, TMS): δ 192.1, 159.1, 137.5, 136.5, 130.1, 128.8, 128.7, 128.5, 128.3, 124.2, 122.2, 61.6, 58.4, 41.6, 20.2; IR: $\bar{\nu}$ = 3511 (O-H), 2845 (C-H), 1679 (C=O), 1473 (Ar-C=C), 1608 (Ar-C=C) cm^{-1}; MS: *m/z* (ESI) 461 $[M+H]^+$; elemental analysis calcd. (%) for $C_{28}H_{32}N_2O_4 \cdot 0.1CH_2Cl_2$: C 71.95, H 6.92, N 5.97; found: C 72.10, H 7.01, N 6.01.

L"o (Precursor for L"): 3,3'-[1,3-phenylenebis[methylene(methylimino)methylene]]bis[2-hydroxy-5-methylbenzaldehyde]-1,1'-dioxime

A solution of hydroxylamine hydrochloride (1.21 g, 17.4 mmol) in ethanol (240 mL) was neutralised with a solution of potassium hydroxide (0.970 g, 17.4 mmol) in ethanol (240 mL). The filtered solution was added slowly dropwise to a solution of **L"a** (4.00 g, 8.68 mmol) in chloroform : ethanol (20 : 380 mL) over 30 minutes. The resulting solution was stirred for 48 hours at RT. The pale yellow solution was concentrated *in vacuo* affording an oil, which was redissolved in chloroform (300 mL). This solution was washed with deionised water (3 x 250 mL) and the combined organic layers were dried over anhydrous sodium sulfate, filtered and concentrated *in vacuo* to afford a pale-yellow solid. R_f = 0.74 (Triethylamine/Ethyl acetate, 1:9) (3.84 g, 90%). ^{1}H NMR (500 MHz, $CDCl_3$, TMS): δ 8.39 (s, 2H, C*H*N), 7.32 (t, J = 7.1 Hz, 1H, Ar-*H*), 7.30 (s, 1H, Ar-*H*), 7.26 (d, J = 7.7 Hz, 4H, Ar-*H* (σ-oxime)), 7.22 (s, 2H, Ar-*H*), 6.93 (d, J = 1.1 Hz, 2H, Ar-*H* (σ-oxime)), 3.69 (s, 4H, Ar-CH_2N), 3.63 (s, 4H, Ar-CH_2N), 2.26 (s, 6H, NCH_3), 2.25 (s, 6H, Ar-CH_3); ^{13}C NMR (125.7 MHz, $CDCl_3$, TMS): δ 154.1, 148.3, 137.5, 131.5, 130.3, 128.7, 128.5, 128.0, 127.2, 123.2, 118.1, 61.6, 58.9, 41.5, 20.4; IR: $\bar{\nu}$ = 2975 (C-H), 1618 (C=N), 1467 (-CH_2), 1288 (C-O), 1018 (N-O), 734 (Ar-H) cm^{-1}; MS: *m/z* (ESI) 492 $[M+H]^+$; elemental analysis calcd. (%) for $C_{28}H_{34}N_4O_4 \cdot 0.5C_6H_{15}N$: C 68.80, H 7.73, N 11.65; found: C 68.93, H 7.58, N 11.54.

L"'a (Precursor for L"'o): 3-Methylene-(*N*-benzyl-β-alanine-methylester)-5-*tert*-butyl-2-hydroxybenzaldehyde

Solutions of **1b** (20.5 g, 75.4 mmol) and **3** (13.5 g, 75.4 mmol) both in chloroform (100 mL) were added dropwise to a stirred solution of triethylamine (7.62 g, 75.4 mmol) in chloroform (100 mL). The resulting yellow solution was stirred for 24 hours at RT. The solution was washed with deionised water (3 x 100 mL) and the combined organic layers were dried over anhydrous magnesium sulfate, filtered and concentrated *in vacuo* to afford a dark yellow oil. R_f = 0.75 (Hexane/Diethyl ether, 1:1); (24.2 g, 87%). ^{1}H NMR (500 MHz, $CDCl_3$): δ 10.19 (s, 1H, C*H*O), 7.55 (d, J = 2.5 Hz, 1H, Ar-*H*(σ-amine)), 7.50 (d, J = 2.5 Hz, 1H, Ar-*H*(σ-oxime)), 7.36-7.28 (m, 5H, C_6H_5-CH_2), 3.75 (s, 2H, C_6H_5-CH_2), 3.66 (s, 2H, Ar-CH_2NBn), 3.64 (s, 3H, O*Me*), 2.89 (t, J = 7.3 Hz, 2H, NBn-*CH*$_2$-CH_2), 2.58 (t, J = 7.3 Hz, 2H, CH_2-*CH*$_2$-COO), 1.31 (s, 9H, ^{t}*Bu*); ^{13}C NMR (176 MHz, $CDCl_3$): δ 193.5, 172.5, 158.6, 142.2, 137.5, 133.9, 129.2, 128.5, 127.5, 126.0, 124.8, 121.4, 58.3, 53.9, 51.7, 49.3, 34.1, 32.2, 31.3; IR: $\bar{\nu}$ = 2956 (C-H), 1737 (C=O), 1679 (C-H), 1651 (C=C), 1454 (C-H), 1364 (O-H), 1215 (C-O), 1028 (C-N) cm^{-1}; MS: *m/z* (ESI) 384 $[M+H]^+$; UV/Vis (ε, L/mol cm) in MeOH: 339.5 (3455), 260.0 (8766), 205.5 (22883).

L"'o (Precursor for L"'): 3-Methylene-(*N*-benzyl-β-alanine-methylester)-5-*tert*-butyl-2-hydroxybenzaldehyde oxime

A solution of hydroxylamine hydrochloride (0.29 g, 4.16 mmol) in ethanol (50 mL) was neutralised with a solution of potassium hydroxide (0.23 g, 4.16 mmol) in ethanol (50 mL). The filtered solution was added slowly dropwise to a solution of **L"'a** (1.60 g, 4.16 mmol) in ethanol (50 mL) over 30 minutes. The resulting solution was stirred for 24 hours at RT. The pale yellow solution was concentrated *in vacuo* affording an oil, which was redissolved in chloroform (50 mL). This solution was washed with deionised water (3 x 50 mL) and the combined organic layers were dried over anhydrous magnesium sulfate, filtered and concentrated *in vacuo* to afford a pale-yellow oil (1.60 g, 97%). ^{1}H NMR (500 MHz, $CDCl_3$): δ 8.46 (s, 1H, C*H*N), 7.44 (d, J = 2.5 Hz, 1H, Ar-*H* (σ-amime)), 7.35-7.27 (m, 5H, C_6H_5-CH_2), 7.16 (d, J = 2.5 Hz, 1H, Ar-*H* (σ-oxime)), 3.75 (s, 2H, C_6H_5-CH_2), 3.66 (s, 2H, Ar-CH_2-NBn), 3.65 (s, 3H, O*Me*), 2.88 (t, J = 7.3 Hz, 2H, NBn-*CH*$_2$-CH_2), 2.58 (t, J = 7.3 Hz, 2H, CH_2-*CH*$_2$-COO), 1.29 (s, 9H, ^{t}*Bu*); ^{13}C NMR (125.7 MHz, $CDCl_3$): δ 172.5, 153.9,

View Article Online
DOI: 10.1039/C9DT01968E

149.0, 142.0, 136.9, 129.4, 128.5, 128.3, 127.6, 123.6, 122.7, 117.5, 58.1, 55.8, 51.8, 49.0, 34.1, 31.9, 31.4; IR: $\bar{\nu}$ = 3397 (O-H), 2955 (C-H), 1736 (C=O), 1626 (C=N), 1454 (-CH_2), 1393 (^{t}Bu), 1363 (O-H), 1212 (C-O), 1027 (C-N) cm^{-1}; MS: *m/z* (ESI) 399 $[M+H]^+$; UV/Vis (ε, L/mol cm) in MeOH: 315.0 (4135), 261.5 (10090), 214.5 (25835); elemental analysis calcd. (%) for $C_{23}H_{30}N_2O_4$: C 69.15, H 7.82, N 7.01; found: C 68.77, H 7.65, N 6.99.

Complex Syntheses

$[Fe_2(L'+2H)_2](BF_4)_2(MeOH)_4$ (C1)

To the precursor **L'o** (0.125 g, 0.500 mmol) dissolved in MeOH (12.5 mL), was added $Fe(BF_4)_2{\cdot}6H_2O$ (0.169 g, 0.500 mmol) dissolved in MeOH (12.5 mL). After full dissolution, pyridine (2 mL) was added to the maroon solution and the mixture was left to stir for three hours at RT. The mixture was filtered, and the filtrate was left to slowly evaporate. X-ray quality crystals were produced after two weeks. The crystals were crushed and dried prior to further analysis (0.091 g, 49%); elemental analysis calc. (%) for $C_{52}H_{68}B_4F_{10}Fe_2N_8O_{14}{\cdot}8H_2O$: C 41.14, H 5.58, N 7.38; found: C 40.93, H 5.31, N 7.63.

$[Fe_3(L''+4H)(OH)_2(Py)_2](BF_4)_2(H_2O)_2(Py)_2$ (C2)

To the precursor **L"o** (0.245 g, 0.500 mmol) dissolved in MeOH (12.5 mL), was added $Fe(BF_4)_2{\cdot}6H_2O$ (0.337 g, 1.00 mmol) dissolved in MeOH (12.5 mL). After full dissolution, pyridine (2 mL) was added to the maroon solution and the mixture was left to stir for three hours at RT. The mixture was filtered, and the filtrate was left to slowly evaporate. X-ray quality crystals were produced after two weeks. The crystals were crushed and dried prior to further analysis (0.078 g, 28%); elemental analysis calc. (%) for $C_{66}H_{76}B_3F_8Fe_3N_{10}O_{12}{\cdot}4H_2O$: C 48.77, H 5.21, N 8.62; found: C 48.78, H 5.10, N 8.90.

$[Cu_2(L'''+H)_2Cl_2]$ (C3)

To the precursor **L'"o** (0.338 g, 0.85 mmol) in methanol (10 mL) was added $Cu(BF_4)_2{\cdot}6H_2O$ (0.293 g, 0.85 mmol) and ammonium chloride (0.045 g, 0.85 mmol), both in methanol (10 mL). The dark green solution was left to stir at RT for 30 minutes. Isolation of the complex was achieved by the diffusion of diethyl ether into the reaction solution. X-ray quality crystals were produced after two weeks. The crystals were crushed and dried prior to further analysis (0.230 g, 24%); ^{19}F NMR (30 MHz, $CDCl_3$, Trifluoroethanol): δ -150.4; IR: $\bar{\nu}$ = 3324 (N-H), 2965 (C-H), 1738 (C=O), 1565 (C=N), 1462 (C-H), 1267 (C-O), 1044 (C-N) cm^{-1}; MS: *m/z* (ESI) 1001 $[M+H]^+$; Uv/Vis (ε, L/mol cm) in MeOH: 348.0 (11991), 298.5 (12068), 207.0 (197674); Conductivity (MeOH): λ = 222 S cm^2 mol^{-1}, a 2:1 electrolyte in the range 210-250 S cm^2 mol^{-1}.

Conflicts of interest

There are no conflicts to declare.

Notes and references

1 J. B. Vincent, G. L. Olivier-Lilley and B. A. Averill, *Chem. Rev.*, 1990.
2 I. A. Cohen, *Struct. Bonding*, 1980, **40**, 1–37.
3 P. L. Jones, J. C. Jeffery, J. A. McCleverty and M. D. Ward, *Polyhedron*, 1997, **16**, 1567–1571.
4 A. Horn, A. Neves, A. J. Bortoluzzi, V. Drago and W. A. Ortiz, *Inorg. Chem. Commun.*, 2001, **4**, 173–176.
5 M. Faiella, C. Andreozzi, R. T. M. de Rosales, V. Pavone, O. Maglio, F. Nastri, W. F. DeGrado and A. Lombardi, *Nat. Chem. Biol.*, 2009, **5**, 882–884.
6 K. Weighardt, K. Pohl, I. Jibril and G. Huttner, *Angew. Chem. Int. Ed.*, 1984, **23**, 77–78.
7 A. L. Barra, P. Debrunner, D. Gatteschi, C. E. Schulz and R. Sessoli, *Europhys. Lett.*, 1996, **35**, 133–138.
8 G. Aromi and E. K. Brechin, *Struct. Bonding*, 2006, **122**, 1–67.
9 E. Rodriguez, M. Gich, A. Roig, E. Molins, N. Nedelko, A. Slawska-Waniewska and A. Szewczyk, *Polyhedron*, 2006, **25**, 113–118.
10 R. S. Forgan, J. E. Davidson, F. P. Fabbiani, S. G. Galbraith, D. K. Henderson, S. A. Moggach, S. Parsons, P. A. Tasker and F. J. White, *Dalton Trans.*, 2010, **39**, 1763–1770.
11 R. S. Forgan, J. E. Davidson, S. G. Galbraith, D. K. Henderson, S. Parsons, P. A. Tasker and F. J. White, *Chem. Commun.*, 2008, 4049–4051.
12 J. L. Bila, M. Marmier, K. O. Zhurov, R. Scopelliti, I. Zivkovic, H. M. Ronnow, N. E. Shaik, A. Sienkiewicz, C. Fink and K. Severin, *Eur. J. Inorg. Chem.*, 2018, 3118–3125.
13 G. Cecot, M. Marmier, S. Geremia, R. D. Zorzi, A. V. Vologzhanina, P. Pattison, E. Solari, T. F. Fadaei, R. Scopelliti and K. Severin, *J. Am. Chem. Soc.*, 2017, **139**, 8371–8381.
14 M. Marmier, G. Cecot, B. F. Curchod, P. Pattison, E. Solari, R. Scopelliti and K. Severin, *Dalton Trans.*, 2016, **45**, 8422–8427.
15 M. Marmier, G. Cecot, A. V. Vologzhanina, J. L. Bila, I. Zivkovic, H. M. Ronnow, B. Nafradi, E. Solari, P. Pattison, R. Scopelliti and K. Severin, *Dalton Trans.*, 2016, **45**, 15507–15516.
16 M. Marmier, M. D. Wise, J. J. Holstein, P. Pattison, K. Schenk, E. Solari, R. Scopelliti and k. Severin, *Inorg. Chem.*, 2016, **55**, 4006–4015.
17 M. Pascu, M. Marmier, C. Schouwey, R. Scopelliti, J. J. Holstein, G. Bricogne and K. Severin, *Chem. Eur. J.*, 2014, **20**, 5592–5600.
18 G. W. Bates, J. E. Davidson, R. S. Forgan, P. A. Gale, D. K. Henderson, M. G. King, M. E. Light, S. J. Moore, P. A. Tasker and C. C. Tong, *Supramol. Chem.*, 2012, **24**, 117–126.
19 R. A. Coxall, L. F. Lindloy, H. A. Miller, A. Parkin, S. Parsons, P. A. Tasker and D. J. White, *Dalton Trans.*, 2003, **0**, 55–64.
20 E. Bill, C. Krebs, M. Winter, M. Gerdan, A. X. Trautwein, U. Floerke, H.-J. Haupt and P. Chaudhuri, *Chem. Eur. J.*, 1997, **3**, 193–201.
21 P. Chaudhuri, M. Winter, P. Fleischhauer, W. Haase, U. Floerke and H.-J. Haupt, *Inorg. Chim. Acta.*, 1993, **212**, 241–249.
22 C. J. Milios, A. Vinslava, W. Wernsdorfer, S. Moggach, S. Parsons, S. P. Perlepes, G. Christou and E. K. Brechin, *J. Am. Chem. Soc.*, 2007, **129**, 2754–2755.

View Article Online
DOI: 10.1039/C9DT01968E

23 C.-I. Yang, K.-H. Cheng, S.-P. Hung, M. Nakano and H.-L. Tsai, *Polyhedron*, 2011, **30**, 3272–3278.
24 S. K. Langley, N. F. Chilton, M. Massi, B. Moubaraki, K. J. Berry and K. S. Murray, *Dalton Trans.*, 2010, **39**, 7236–7249.
25 C. J. Milios, S. Piligkos and E. K. Brechin, *Dalton Trans.*, 2008, 1809–1817.
26 T. C. Stamatatos, D. Foguet-Albiol, C. C. Stoumpos, C. P. Raptopoulou, A. Terzis, W. Wernsdorfer, S. P. Perlepes and G. Christou, *J. Am. Chem. Soc.*, 2005, **127**, 15380–15381.
27 A. R. Stefankiewicz, M. Walesa-Chorab, J. Harrowfield, M. Kubicki, Z. Hnatejko, M. Korabik and V. Patroniak, *Dalton Trans.*, 2013, **42**, 1743–1751.
28 C. Ge, J. Zhang, Z. Qin, P. Zhang, R. Zhang, H. Zhao, Y. Wang and X. Zhang, *Inorg. Chim. Acta.*, 2017, **463**, 134–141.
29 Z. Qin, F. Han, C. Ge, R. Zhang, Y. Zhang and X. Zhang, *Inorg. Chim. Acta.*, 2018, **479**, 36–41.
30 J. Zhang, Z. Ma, H. Zhao, C. Ge, Y. Wang and X. Zhang, *Inorg. Chem. Commun.*, 2016, **65**, 63–67.
31 G. N. Schrauzer, *Chem. Ber.*, 1962, **95**, 1438–1445.
32 S. Khanra, T. Weyhermuller, E. Bill and P. Chaudhuri, *Inorg. Chem.*, 2006, **45**, 5911–5923.
33 S. S. Tandon, S. D. Bunge, S. A. Toth, J. Sanchiz, L. K. Thompson and J. T. Shelley, *Inorg. Chem.*, 2015, **54**, 6873–6884.
34 J. M. Thorpe, R. L. Beddoes, D. Collison, C. D. Garner, M. Helliwell, J. M. Holmes and P. A. Tasker, *Angew. Chem. Int. Ed.*, 1999, **38**, 1119–1121.
35 K. Mason, J. Chang, E. Garlatti, A. Prescimone, S. Yoshii, H. Nojiri, J. Schnack, P. A. Tasker, S. Carretta and E. K. Brechin, *Chem. Commun.*, 2011, **47**, 6018–6020.
36 I. Vasilevsky, N. J. Rose and R. E. Stenkamp, *Acta Crystallogr., Sect. B: Struct. Sci.*, 1992, **B48**, 444–449.
37 C. A. Coulson and T. W. Dingle, *Acta Crystallogr., Sect. B*, 1968, **24**, 153–155.
38 T. Steiner, *Angew. Chem. Int. Ed.*, 2002, **41**, 48–76.
39 K. Mason, J. Chang, A. Prescimone, E. Garlatti, S. Carretta, P. A. Tasker and E. K. Brechin, *Dalton Trans.*, 2012, **41**, 8777–8785.
40 M. Wenzel, R. S. Forgan, A. Faure, K. Mason, P. A. T. adn S. Piligkos, E. K. Brechin and P. G. Plieger, *Eur. J. Inorg. Chem.*, 2009, 4613–4617.
41 M. J. Prushan, A. W. Addison and R. J. Butcher, *Inorg. Chim. Acta.*, 2000, **300**, 992–1003.
42 K. K. Nanda, A. W. Addison, N. Paterson, E. Sinn, L. K. Thompson and U. Sakaguchi, *Inorg. Chem.*, 1997, **37**, 1028–1036.
43 C. P. Raptopoulou, Y. Sanakis, A. K. Boudalis and V. Psycharis, *Polyhedron*, 2005, **24**, 711–721.
44 E. Murad and J. Cashion, *Moessbauer Spectroscopy of Environmental Materials and Their Industrial Utilization*, Kluwer Academic, 2004.
45 S. Chandra and S. D. S. Sangeetika, *Spectrochim. Acta, Part A*, 2003, **59A**, 755–760.
46 Z. A. Siddiqi, M. Shahid, M. Khalid, S. Noor and S. Kumar, *Spectrochim. Acta A Mol. Biomol. Spectrosc.*, 2010, **75**, 61–68.
47 D. Collison and A. K. Powell, *Inorg. Chem.*, 4735–4746.
48 V. H. Crawford, H. W. Richardson, J. R. Wasson, D. J. Hodgson and W. E. Hatfield, *Inorg. Chem.*, 1976, **15**, 2107.
49 L. Merz and W. Hasse, *J. Chem. Soc., Dalton Trans.*, 1980, 875.
50 Rigaku Americas Corporation, The Woodlands, Texas, *Crystal Clear*, 1st edn, 2005.
51 Rigaku Corporation, Tokyo, *PROCESS-AUTO*, 1998.
52 O. V. Dolomanov, L. J. Bourhis, R. J. Gildea, J. A. Howard and H. Puschmann, *J. Appl. Cryst.*, 2009, **42**, 339–341.
53 G. M. Sheldrick, *Acta Crystallogr., Sect. A*, 2008, **64**, 112–122.
54 G. M. Sheldrick, *Acta Crystallogr., Sect. C. Struct. Chem.*, 2015, **71**, 3–8.
55 L. P. G. Chapuis, *J. Appl. Cryst.*, **40**, 786–790.
56 L. Palatinus and G. Chapuis, *J. Appl. Cryst.*, 2007, **40**, 786–790.
57 L. Palatinus and A. V. der Lee, *J. Appl. Cryst.*, 2008, **41**, 975–984.
58 L. Palatinus, S. J. Prathapa and S. V. Smaalen, *J. Appl. Cryst.*, 2012, **45**, 575–580.
59 A. Spek, *J. Appl. Cryst.*, 2015, **71**, 9–18.
60 R. Aldred, R. Johnston, D. Levin and J. Neilan, *J. Chem. Soc., Perkin Trans. 1*, 1994, 1823–1831.
61 Q. Wang, C. Wilson, A. J. Blake, S. R. Collinson, P. A. Tasker and M. Schroeder, *Tetrahedron Lett.*, 2006, **47**, 8983–8987.
62 P. Meier, F. Broghammer, K. Latendorf, G. Rauhut and R. Peters, *Molecules*, 2012, **17**, 7121–7150.
63 J. R. Stevens and P. G. Plieger, *Dalton Trans.*, 2011, **40**, 12235–12241.
64 J. Cruz-Huerta, Carillo-Morales, E. Santacruz-Juarez, I. F. Hernandez-Ahuactzi, J. Escalante-Garcia, J. A. Godoy-Alcantar, H. Hopfl, H. Morales-Rojas and M. Sanchez, *Inorg. Chem.*, 2008, **47**, 9874–9885.

View Article Online
DOI: 10.1039/C9DT01968E

Table of Contents for the paper: New salicylaldoximato-borate ligands resulting from anion hydrolysis and their respective copper and iron complexes.

Image:

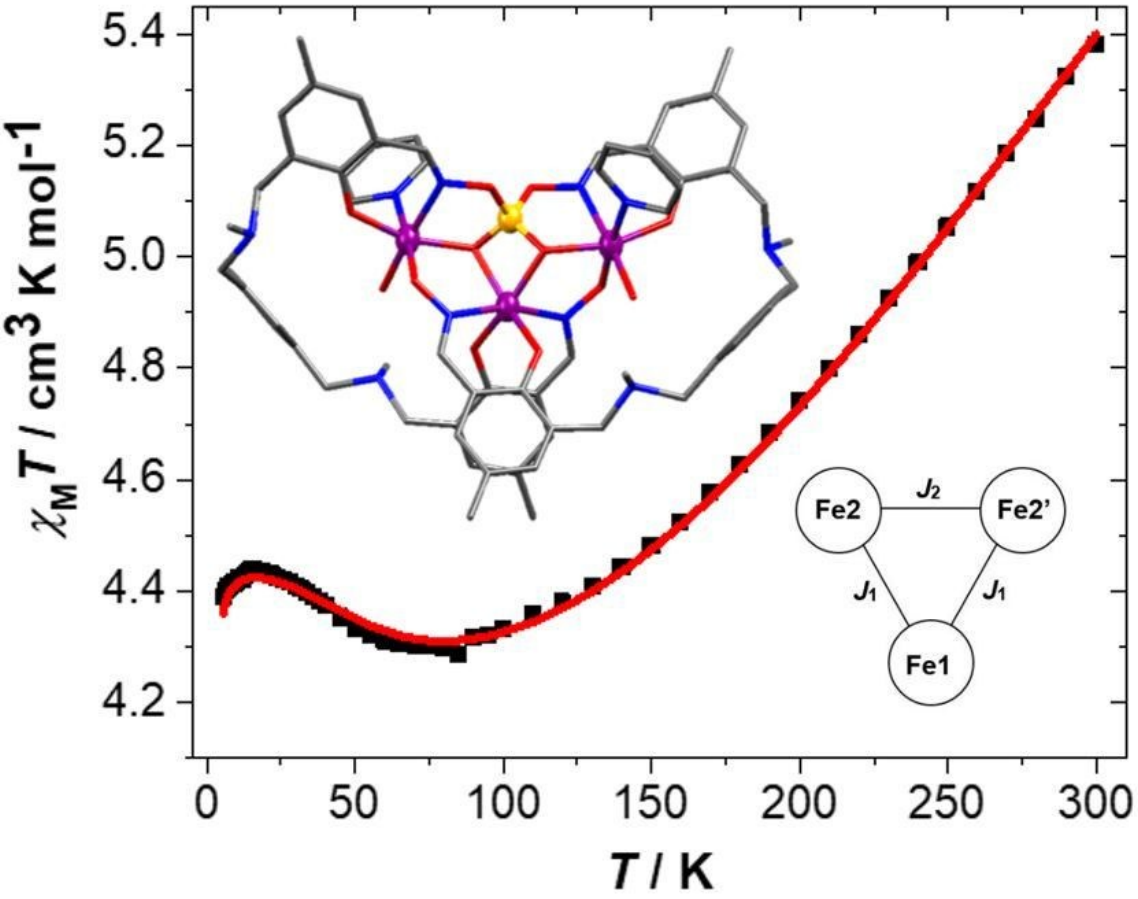

Description: The magnetism, Mössbauer, and structural properties of a series of borate appended ligands are described.